Identification of separate isoenergetic routes for vibrational energy flow in *p*-fluorotoluene

Adrian M. Gardner,[a] Laura E. Whalley, David J. Kemp, William D. Tuttle, and Timothy G. Wright[b]

School of Chemistry, University of Nottingham, University Park, Nottingham NG7 2RD, UK

[a] Present Address: Stephenson Institute for Renewable Energy, University of Liverpool, L69 7ZF, UK

[b] Tim.Wright@nottingham.ac.uk

Abstract

A deceptively simple feature in the $S_1 \leftarrow S_0$ spectrum of *p*-fluorotoluene (*p*FT), 1013 cm^{-1} above the origin, is studied using both zero-electron-kinetic-energy (ZEKE) and two-dimensional laser-induced fluorescence (2D-LIF) spectroscopy. It is found to consist of a cornucopia of overlapped transitions to eigenstates that arise from numerous interacting levels. Significant variation in the activity is seen employing both the ZEKE and 2D-LIF techniques. Detailed insight into the complicated spectra can be achieved, owing to the large number of vibrational wavenumbers that have been previously determined for the S_0, S_1 and D_0^+ states, summarized herein. It is found that the activity is dominated by two overtones, which are individually interacting with other levels, so providing largely independent routes for vibrational energy flow at the same internal energy. Additionally, other weak features located 900–1050 cm^{-1} above the origin are examined.

I. INTRODUCTION

When chemical bonds are formed or broken, excess energy is often deposited locally; further, photoabsorption, photoemission, collision, internal conversion and intersystem crossing can all lead to high amounts of vibrational energy, which again can be localized in a molecule. What happens to this energy is of key importance in understanding the subsequent stability and reactivity of the excited molecule: this is the area of vibrational energy redistribution.[1] Understanding the details of such couplings at high internal energy is nigh on impossible, owing to the enormous numbers of coupled levels; however, although at low internal energy, such couplings can be surprisingly complicated, this is a more tractable problem. We present such a situation in the present work.

Internal energy flow through a molecule is facilitated by the efficient coupling of vibrational, torsional and rotational motions. The role of such couplings depend upon the quantum number changes involved, and the efficiency with which different motions can be coupled; these couplings are usually the highest for relatively small changes in the various quantum numbers, and can be starkly different for different vibrational motions. Further, the couplings often have a hierarchy, with initial, strong couplings leading to the opening up of further couplings, which can lead to a highly interlinked set of coupled levels, often referred to as the tier model.[1] Earlier work on *p*-fluorotoluene (*p*FT) by Parmenter and coworkers,[2,3,4,5,6,7,8] and others[9,10,11,12] has been significantly extended in recent work by the Lawrance group (Flinders University, Adelaide), the Reid group (Nottingham) and ourselves, focusing on vibrational anharmonic and vibration-torsional ("vibtor") coupling[13,14,15,16,17,18,19,20,21,22] as well as other substituted methylbenzenes. [15,20,23,24,25,26,27,28,29,30,31,32] Key to unravelling the often-complicated coupling has been monitoring activity from different intermediate levels by recording zero-electron-kinetic-energy (ZEKE) and/or two-dimensional laser-induced fluorescence (2D-LIF) spectra. As a result of this work, now many gas-phase, experimental vibrational wavenumbers are known for the ground state neutral (S_0), the first excited state (S_1) and the ground state cation (D_0^+). These will prove invaluable in the assignment of the particularly complicated feature that is the focus of the present work, which is the last in a series of papers from our group on the spectroscopy of the *p*FT molecule using the ZEKE and 2D-LIF techniques.

Here, we concentrate on the feature that appears at 1013 cm^{-1} above the origin in the $S_1 \leftarrow S_0$ spectrum of *p*FT, but we also examine a number of weak bands that lie in the range 900–1050 cm^{-1}, identified using resonance-enhanced multiphoton ionization (REMPI). As will be seen, although the 1013 cm^{-1} feature looks like a simple band, albeit broadened, in fact it originates from a surprising number of overlapping transitions, involving eigenstates that arise from a number of interacting levels.

II. EXPERIMENTAL

The ZEKE[13] and 2D-LIF[19] apparatuses are the same as those employed recently. In each case, the vapour above room temperature *p*-fluorotoluene (99% purity, Alfa Aesar) was seeded in ~5 bar of Ar and the gaseous mixture passed through a General Valve pulsed nozzle (750 μm, 10 Hz, opening time of 180–210 μs) to create a free jet expansion.

For the 2D-LIF spectra, the expansion was intersected at *X*/*D* ~20 by the frequency-doubled output of a single dye laser (Sirah CobraStretch), operating with Coumarin 503. The fluorescence was collected, collimated and focused onto the entrance slits of a 1.5 m Czerny-Turner spectrometer (Sciencetech 9150) operating in single-pass mode, dispersed by a 3600 groove/mm grating, and ~300 cm^{-1} windows of the dispersed fluorescence collected by a CCD camera (Andor iStar DH334T). At a fixed grating angle of the spectrometer, the excitation laser was scanned, and at each excitation wavenumber the camera image was accumulated for 2000 laser shots. This allowed a plot to be produced of fluorescence intensity versus both the excitation laser wavenumber and the wavenumber of the emitted and dispersed fluorescence, termed a 2D-LIF spectrum. [33,34]

For the REMPI/ZEKE work, the focused, frequency-doubled outputs of the two dye lasers (Sirah CobraStretch) were overlapped spatially and temporally and passed through a vacuum chamber coaxially and counterpropagating. Here, they intersected the free jet expansion of *p*FT in Ar between two biased electrical grids located in the extraction region of a time-of-flight mass spectrometer, which was employed in the REMPI experiments. These grids were also used in the ZEKE experiments by application of pulsed voltages, giving typical fields (*F*) of ~10 V cm^{-1}, after a delay of up to 2 μs. (This delay was minimized while avoiding the introduction of excess noise from the prompt electron signal.) The resulting ZEKE bands had widths of ~5-7 cm^{-1}. Electron and ion signals were recorded on separate sets of microchannel plates. The excitation laser operated with Coumarin 503, while the ionization laser operated with Pyrromethene 597. The fundamental outputs produced by each dye laser were frequency doubled.

III. RESULTS AND ASSIGNMENTS

A Nomenclature and labelling

We shall employ the D_i labels from Ref. 40 (see Table 1). In previous work, Wilson[35]/Varsányi[36] or Mulliken[37]/Herzberg[38] notations have been employed for the vibrations of *p*FT, but these are not appropriate.[39,40] In other papers, we have provided correlations between the various sets of labels that have been used.[18,21]

Since the G_{12} molecular symmetry group (MSG) is appropriate for vibtor levels in *p*FT, we shall use these symmetry labels throughout. In addition, torsional levels will be labelled via their m quantum number, which has been used and explained in previous work. [16,23,26,27,28,] Under the free-jet expansion conditions employed here, almost all of the molecules are expected to be cooled to their zero-point vibrational level and thus the $S_1 \leftarrow S_0$ pure vibrational excitations are expected to be almost entirely from this level. In contrast, owing to nuclear-spin and rotational symmetry, the molecules can be in one of the m = 0 or m = 1 torsional levels.[23,41] Correspondence between the C_{2v} point group labels and the G_{12} MSG ones are given in Table 2. In calculating direct products, it is useful to note that the G_{12} MSG and the D_{3h} point group are isomorphic.

Anharmonic coupling allows vibrations close in wavenumber, and of the same overall symmetry, to interact. The interacting levels are termed zero-order states (ZOSs) and new eigenstates are formed from these.[38] The simplest example of two interacting states is the classic Fermi resonance (FR).[42] For molecules that contain a hindered internal rotor, vibration-torsional coupling can occur, and the ZOSs can then also be torsional or vibtor levels. Such interactions result in the formation of eigenstates that contain a range of motions that can facilitate delocalization of energy through a molecule. Efficient coupling is only expected for small changes, $\Delta v \approx 3$, of the vibrational quantum number. By Δv we mean the number of quanta difference between two vibrational levels. As an example, in previous work[22] we have discussed the interaction between 9^1 and 29^2: these differ by three quanta, one in D_9 and two in D_{29}, giving a Δv value of 3 overall. The strength of coupling involving changes in the torsional quantum number, Δm, is in the order 0, ±3 or ±6 in descending order of likely strength. [16,23,27,43,44]

In electronic spectroscopy, a ZOS can be bright (i.e. it has a significant transition intensity) or dark (i.e. it has no, or a very small, transition intensity); these are often termed a zero-order bright (ZOB) state

and a zero-order dark (ZOD) state, respectively. As a result of coupling, the resulting eigenstates will be composed of mixtures of ZOB and ZOD state character and so their transitions can be observed in a spectrum, by virtue of the ZOB character.

We shall generally omit the lower level when designating excitations, since it will be clear from the jet-cooled conditions; similarly, for emissions, we shall omit the upper level, as that will be obvious from the excitation and context. In the usual way, vibrational transitions will be indicated by the cardinal number, *i*, of the D_i vibration, followed by a super/subscript specifying the number of quanta in the upper/lower states, respectively; torsional transitions will be indicated by *m* followed by its value. Finally, vibtor transitions will be indicated by a combination of the vibrational and torsional transition labels. If no *m* values are specified, then the transition label refers to transitions involving both $m = 0$ and $m = 1$, whose transition wavenumbers are expected to be coincident at the present resolution.

The wavenumbers of the levels will be given with respect to the relevant zero-point level in each electronic state, but noting that some excitations will originate from the $m = 1$ level in S_0 and those internal energies are given with respect to that level, as usual. The $S_1 \leftrightarrow S_0$ origin is located at 36860.0 cm^{-1} (Ref. 17). The most intense transition is generally expected to be that for which no change in the vibrational, or both vibrational and torsional, quantum numbers occurs; these will be designated as $\Delta v = 0$ or $\Delta(v, m) = 0$ transitions, respectively. As has become common usage, we will generally refer to a level using the notation of a transition, with the level indicated by the specified quantum numbers, with superscripts indicating levels in the S_1 state and subscripts indicating levels in the S_0 state. Since we will also be referring to levels in the ground state cation, D_0^+, we shall indicate those levels in the text with superscripts and with a single preceding superscripted + sign. Also, the eigenstates will often be referred to by the dominant contribution from one of the ZOSs, with the context implying if an admixture of other ZOSs is present. 2D-LIF band positions will be indicated by a pair of (excitation, emission) wavenumbers, and the corresponding transitions similarly.

B. The $S_1 \leftarrow S_0$ spectrum

In Figure 1, we show an overview REMPI spectrum of the $S_1 \leftarrow S_0$ transition in *p*FT in the range 0 – 1250 cm^{-1}. In the spectrum are indicated: the torsional region; a set of bands at ~400 cm^{-1} dominated by 14^2, 29^1 and 11^1;[13,16,17,21] and another at ~800 cm^{-1} dominated by a pair of levels that largely comprise a Fermi resonance (FR) between 9^1 and 29^2.[18,22,45,46] To slightly higher wavenumber, there is

a feature at ~845 cm^{-1} dominated by the 18^2 transition, but there are significant interactions with several vibtor levels.[19] Combinations of the levels in the ~400 cm^{-1} and ~800 cm^{-1} regions, located close to 1200 cm^{-1}, have also recently been studied using ZEKE and 2D-LIF spectroscopy.[20,47]

The bands that are the subject of the present work are located in the range 900–1050 cm^{-1}, and the particular emphasis is on the feature at 1013 cm^{-1}. An expanded view of this region of the REMPI spectrum is indicated in Figure 1. Previous work has allowed the determination of a significant number of the vibrational wavenumbers for the S_0, S_1 and D_0^+ states, and these are tabulated in Table 1 with the most recent values indicated. We shall use these wavenumbers to help in the assignment of both the ZEKE and 2D-LIF spectra. Also pertinent will be the wavenumbers of the torsional and low-wavenumber vibration-torsional levels determined in the S_0 and S_1 states by Gascooke et al.[17]

C. The 1013 cm^{-1} feature

1. Overview

In Figure 1, it can be seen that the feature at ~1013 cm^{-1} is relatively broad, indicating that it is made up of multiple transitions. Additionally, there are two weak bands to slightly higher wavenumber. We have recorded ZEKE spectra at different excitation points across the 1013 cm^{-1} feature and these are shown in Figure 2. Expanded views of the central region of these spectra are displayed in Figure 3. It is clear that there are numerous bands in these spectra and that their relative intensities change as the band is traversed. Although the main $\Delta v = 0$ bands are in the centre of the spectral range shown (see Figure 3), these are severely overlapped and so not always easy to discern clearly. Further, if an eigenstate is formed from the interaction of many levels, then the ZEKE activity is likely to be spread over many bands. The congestion within the $\Delta v = 0$ region is thus indicative of significant interaction between ZOSs. As will shortly be seen, key aspects of the spectra that facilitate assignments are the bands in the low-wavenumber region (0–800 cm^{-1}); these bands arise from $\Delta v < 0$ changes in vibrational quantum number. We have found in previous work that the $\Delta v < 0$ bands, whose intensity can arise from contributions from a number of different transitions, are often diagnostic in establishing the main levels involved, and this is greatly aided by their appearance in a relatively uncongested region of the spectrum.

In Figure 4, we show an overview of the 2D-LIF spectrum recorded across the 1013 cm^{-1} feature with the main activity being highlighted in Figure 5. It may be immediately seen that there is a wealth of activity across the spectrum, with close inspection showing that there are columns of activity at different excitation wavenumbers; this is consistent with there being multiple contributions to the spectrum. (Recall that a vertical slice through the image at a particular excitation wavenumber constitutes a conventional dispersed fluorescence spectrum, while an integration of the image vertically constitutes a conventional LIF spectrum, assuming all of the main activity is present in the 2D-LIF image.[33]) Since the spectrum is so rich in structure, it is difficult both to extract and to indicate the assignments of the various features. To aid in this, we have integrated the spectrum horizontally, and present this on the right-hand side of the 2D-LIF spectrum in each of Figure 4 and Figure 5. The assignments of the main levels involved in the S_1 eigenstates are indicated at the top of the 2D-LIF spectrum in Figure 4, and the assignments of the main emission bands are indicated on the integrated traces in Figure 4 and Figure 5 – these will be discussed below, in tandem with the ZEKE spectra.

We first address what levels we expect to be located in this spectral region. Table 1 contains the calculated and experimental wavenumbers for the harmonic normal modes in the S_1 state. From these, we have calculated all of the combinations and overtones that could contribute to this spectral range. These are tabulated in Table 3, where both a_1' and a_1'' symmetry modes have been included, with the former being those that are (symmetry-) Franck-Condon (FC)-allowed, and the latter those that are Herzberg-Teller (HT)-allowed. (Note that these values have generally simply been obtained from summing the wavenumbers of the individual D_i vibrations, with no account of anharmonicity nor other interactions having been included; the exceptions are for 20^2 and $14^120^130^1$ in the S_1 state, where the experimental values were used, since there is significant anharmonicity for those levels.)

A perusal of Table 3, while examining the ZEKE and 2D-LIF spectra, quickly establishes that the two main contributors to the 1013 cm^{-1} feature are the overtones, 17^2 and 13^2. Although the two fundamentals are of different symmetry, a_2'' and a_2', respectively, the overtones are both a_1'. There are also clearly other combination bands (Table 3), but no fundamentals are expected to be present in this region (Table 1). One likely set of combinations is the levels that give rise to the bands at ~400 cm^{-1} (14^2, 29^1 and 11^1) each in combination with 30^2, 17^120^1 or $14^120^130^1$ (these latter three transitions are overlapping); the other is the levels that appear at ~800 cm^{-1} (9^1 and 29^2) each in combination with 20^2 – see Figure 6. These levels all have the possibility to interact with each other, and/or with the 13^2 and/or 17^2 levels. Since the levels that give rise to transitions with significant intensity will produce the most straightforwardly identifiable features in the ZEKE and 2D-LIF spectra, in Table 3 we have

also tabulated the expected wavenumbers for the corresponding overtone and combination bands in the S_0 and D_0^+ states (simply obtained from addition of the individual wavenumbers).

2. Main activity

In the 2D-LIF spectrum (Figure 4 and Figure 5), an intense band is seen at (1014, 1629) cm^{-1}, and is assigned as the Δv = 0 (13^2, 13_2) transition. The 17_2 emission band is broad along the excitation direction, and appears to contain at least two overlapping contributions. The main band centres are estimated at (1011, 1393) cm^{-1} and (1014, 1393) cm^{-1}, with the latter being slightly more intense. It will be confirmed later that the latter band can assigned as the Δv = 0 band. Taking into account anharmonicity, both of these assignments are in line with the calculated and previous experimental values for D_{13} and D_{17} in the S_0 and S_1 states (see Table 1). We note that the essentially coincident S_1 values for these two overtones suggests that they are unlikely to be interacting significantly (via a Darling-Dennison resonance[48]), since this would lead them to move apart in wavenumber. A possible explanation for this is the different atomic motions, as expected for the different symmetries of the fundamentals (see Ref. 40 for the normal mode diagrams); additionally, this would involve a Δv = 4 coupling term.

If we now look at the ZEKE spectra presented in Figure 2, we can see that there is a clear $^+17^2$ band and that its intensity variation across the excitation wavenumber region is in line with the 2D-LIF feature in Figure 5, confirming its assignment. The wavenumber for the $^+17^2$ band of 1368 cm^{-1} is in line with the calculated and experimental values (Table 1). Similarly, a clear $^+13^2$ band can be seen, at 1548 cm^{-1}, and this is also in line with the values in Table 1. The intensity variation of this band, when exciting across the 1013 cm^{-1} feature, is also consistent with that of the corresponding band in the 2D-LIF spectrum, which we shall now discuss.

3. Main interactions

We now examine the intensity profile of the 13_2 band in the 2D-LIF spectrum – see Figure 5. As well as the main Δv = 0 band, this can be seen to have a secondary maximum at (1009, 1629) cm^{-1}. Looking at the rest of the 2D-LIF image, it can be seen that there is band with a maximum at (1009, 1381) cm^{-1}, and this may be assigned as the Δv = 0 band ($13^1 20^1 29^1$, $13_1 20_1 29_1$). The emission at this wavenumber may be seen to have two other areas of activity, one is at (1014, 1381) cm^{-1} and the other is at (1017,

1381) cm^{-1}; we assign the first of these as (13^2, $13_1 20_1 29_1$). The evidence suggests that 13^2 is the ZOB state, and that this couples to $13^1 20^1 29^1$ through a $\Delta v = 3$ term. The emission at 1381 cm^{-1} extends over a large portion of the region shown in Figure 5, which is only partially reflected in the 13_2 profile, indicating that $13^1 20^1 29^1$ undergoes further couplings that are not directly available to 13^2. One such coupling is to $20^2 29^2$, suggesting that the (1017, 1381) cm^{-1} feature largely arises from ($20^2 29^2$, $13_1 20_1 29_1$). This assignment is supported both by the correspondence in excitation position with that expected for $20^2 29^2$, and somewhat by the 20_2 intensity profile shown in Figure 5. The situation is complicated by the fact that $9^1 20^2$ and $20^2 29^2$ are expected to be in FR, as are 9^1 and 29^2 (Ref. 22), and also that the emission intensities from the eigenstates composed of 9^1 and 29^2, were unusual. Additionally, it was concluded that it was possible that the corresponding 9^1 and 29^2 levels may be interacting in S_0 and/or D_0^+. [22] With these, and the additional interactions with $20^2 29^2$, the $9_1 20_2$ and $20_2 29_2$ emission profiles are not necessarily expected to mimic closely those of the 9_1 and 29_2. (It is also probable that 20_2 emission also arises from other levels.)

In summary, the evidence suggests that the 13^2 level is a ZOB state, which couples strongly to $13^1 20^1 29^1$; this latter level is strongly coupled to $20^2 29^2$, and that is coupled to $9^1 20^2$. All of these are $\Delta v = 3$ interactions. Thus, 13^2 is indirectly coupled to $20^2 29^2$ (and $9^1 20^2$), explaining the weak activity at (1018, 1629) cm^{-1}, with the aforementioned (1009, 1629) cm^{-1} band being assigned to ($13^1 20^1 29^1$, 13_2). These interactions will form a set of eigenstates made up of admixtures of these ZOSs and are summarized in Figure 7.

Now referring to the ZEKE spectra in Figure 2 and Figure 3, the above analysis is confirmed, with a strong $^+13^1 20^1 29^1$ band when exciting at 1008 cm^{-1}, whose intensity dies away when exciting towards the centre of the band; this then grows in at around 1018 cm^{-1}. Similarly, the $^+20^2$ band rises in intensity at 1019 cm^{-1}, supporting the presence of combination bands involving 20^2 in the S_1 state at this wavenumber. Moreover, an intense, broad ZEKE feature that appears at ~1051 cm^{-1} – consistent with its containing contributions from $^+9^1 20^2$ and $^+20^2 29^2$. Furthermore, a weak $^+13^1$ band is seen, in line with 13^1 involvement in the S_1 eigenstates. (This is a symmetry-forbidden band, but in line with observations of $^+14^1$ here, see Figure 2, and our previous work.)

We now come back to the 17_2 2D-LIF feature, which consists of emission at 1393 cm^{-1}. It may be seen from Figure 5 that the red side of the 17_2 intensity profile (1011, 1393) cm^{-1} lines up with the maximum in the $14_1 17_1 30_1$ emission, whose $\Delta v = 0$ band is located at (1011, 1419) cm^{-1}. This suggests a $\Delta v = 3$ interaction between 17^2 and $14^1 17^1 30^1$; this is supported by the weak cross-activity seen around

(1014, 1419) cm^{-1}, assignable as ($14^1 17^1 30^1$, 17_2) Further, the close-lying $14_2 30_2$ band, corresponding to emission at 1437 cm^{-1} in the 2D-LIF spectrum, has a similar intensity profile to 17_2. However, a direct coupling is unlikely, since this corresponds to $\Delta v = 6$, and so, analogous to the 13^2 coupling discussed above, we suggest 17^2 couples strongly to $14^1 17^1 30^1$ ($\Delta v = 3$), and that $14^1 17^1 30^1$ couples strongly to $14^2 30^2$ (also $\Delta v = 3$). Thus providing an indirect coupling route between 17^2 and $14^2 30^2$ – see Figure 7. As a result of these couplings the 17^2 character becomes delocalized amongst numerous S_1 eigenstates, as evinced by the broad intensity profile of the 17_2 band; further, the profiles of this and the other bands are likely affected by additional interactions.

We can also see from the ZEKE spectrum in Figure 2, that there is a $^+17^1 20^1$ band, suggesting activity of at least one combination involving $17^1 20^1$. In both the ZEKE and 2D-LIF spectra, it is possible to identify bands associated with such a level: $^+14^2 17^1 20^1$ and $14_2 17_1 20_1$, respectively. The $14^2 17^1 20^1$ level is unlikely to couple strongly to 17^2 directly, since $\Delta v = 4$, but it can couple more strongly to $14^1 17^1 30^1$, for which $\Delta v = 3$. Previously, we have concluded that 11^1 and 14^2 do not interact strongly,[21] in line with the levels being separated by over 10 cm^{-1}, and so although we see weak activity from $11^1 17^1 20^1$, it is likely not from interaction with $14^2 17^1 20^1$. The $11^1 17^1 20^1$ level is $\Delta v = 3$ in relation to 17^2, and the weak activity could be from this. Also, the $11^1 17^1 20^1$ level is $\Delta v = 3$ in relation to $14^1 17^1 30^1$ and so these can couple, but since this level is expected to lie $\gtrsim$ 10 cm^{-1} higher in wavenumber, then we do not expect this to be strong.

Also coincident with 30^2 and $17^1 20^1$ is the level $14^1 20^1 30^1$ (Ref. 18), and the combination of this level with 14^2 should appear in this excitation region – see Figure 6. This would give rise to a $14_3 20_1 30_1$ emission band at 1692 cm^{-1} and a corresponding ZEKE band at 1481 cm^{-1}, and bands consistent with both of these are seen. Furthermore, the $14^3 20^1 30^1$ level is $\Delta v = 3$ in relation to the $14^2 30^2$ level, and so these can be interacting. Higher in wavenumber $11^1 14^1 20^1 30^1$ is expected, and there is a clear emission band at the expected wavenumber (Figure 5) and a plausible ZEKE band (Figure 3). Again, we would not necessarily expect this level to be interacting with $14^3 20^1 30^1$, based on the lack of interaction between 11^1 and 14^2.[21] This discussion of the 17^2 ZOB state and its interactions is summarized in Figure 7. As with the 13^2 levels, these interactions will lead to a set of eigenstates made up of various contributions, but each expected to be dominated by one leading term. As such, the 2D-LIF and ZEKE spectra largely reflect this, as noted above; the cross-activity again helps to deduce the ZOSs that are the main contributors to the eigenstates.

From the 2D-LIF spectra, there is no direct evidence for coupling between the 13^2 and 17^2 levels. This is based upon the differing profiles of the bands (see Figure 5), and also that the $\Delta v = 0$ activity for both 13^2 and 17^2 are close-to-coincident in S_1, whereas the bands would be separated if they were interacting. The location of the $\Delta v = 0$ band for 17^2 is most clearly indicated from the profile of the $14^1 17^1 30^1$ band, whose higher-wavenumber secondary minimum is associated with emission from 17^2. It is clear, and as has been discussed, the profile of the 17^2 band (Figure 5) is suggestive of more wide-ranging interactions, not all of which can be unambiguously deduced from the spectra. An interaction between 13^2 and 17^2 would be $\Delta v = 4$, and so expected to be weaker than the $\Delta v = 3$ interactions that have been put forward in the above discussion. As a consequence, we conclude that there are two, essentially separate, pathways for energy dispersal amongst the $m = 0$ (a_1' symmetry) levels in the 1005–1025 cm^{-1} range; in addition, there will be partner pathways for the corresponding $m = 1$ (e'' symmetry) levels – Figure 7.

In Figure 6, the combination bands that are formed from the contributors to the ~400 cm^{-1} region (14^2, 29^1 and 11^1),[21] each in combination with 30^2, may be seen to fall in this spectral region – see also Table 3. Already mentioned is the $14^2 30^2$ level, which has been concluded to be indirectly coupled to 17^2 (see Figure 7). As reported previously,[13,16,21] the HT-active 29^1 transition is at almost the same wavenumber as 14^2, and so, for example, we might also expect to see activity arising from the counterparts of the abovementioned $14^2 30^2$ and $14^2 17^1 20^1$ bands: $29^1 30^2$ and $17^1 20^1 29^1$ (see Figure 6). The expected, weak emission is indeed seen at (1014, 1032) cm^{-1}, and this also ties in with the observed activity of the $^+29^1 30^2$ ZEKE band, albeit in an overlapped region of the spectrum. We do not expect these levels to interact with the main ZOB states discussed, as they are of different symmetry; however, the $17^1 20^1 29^1$ level could interact with $13^1 17^1$ ($\Delta v = 3$), and there is some weak activity from this level in the spectra, so this is a possible route for energy dispersal amongst a_1'' ($m = 0$) symmetry levels – see Figure 7. Interestingly, we also see emission to $11_1 30_2$ at (1015, 1064) cm^{-1}, but this is attributed to FC activity, and so assigned as ($14^2 30^2$, $11_1 30_2$). This would be in line with activity seen when exciting the ~400 cm^{-1} bands.[21] The ($11^1 30^2$, $11_1 30_2$) $\Delta v = 0$ band is expected at (1030, 1067) cm^{-1} and is outside the regions scanned in this work. As with the $^+20^2$ ZEKE band, we also see the $^+30^2$ ZEKE band at positions where the combination bands including 30^2 are located, confirming their assignment. Again, there will be corresponding routes for the $m = 1$ (e' symmetry) levels.

The 2D-LIF and ZEKE spectra suggest that these two sets of coupled ZOSs, separately involving the 13^2 and 17^2 ZOB states, are the main interactions here, dominating the activity in the 1013 cm^{-1} band. There is, however, another feature in the 2D-LIF spectrum that seems to be independent of these

levels. This is the $15_1 20_3$ band at (1008, 1361) cm^{-1}, with there being no indications of interactions involving the $15^1 20^3$ level. This is similar to the case of the $15^1 20^1$ level discussed in our recent work,[22] which was not interacting with the 9^1 nor 29^2 levels, despite these being in close proximity. The expected $^+15^1 20^3$ ZEKE band is present when exciting at 1008 cm^{-1} (Figure 3), providing further confirmation of the activity of $15^1 20^3$ at this wavenumber, although there is some possible overlap of this band with $^+14^2 30^2$.

On the high-wavenumber side of the 1013 cm^{-1} band, there is a shoulder at 1023 cm^{-1} (see Figure 1) Exciting at this wavenumber gives rise to an emission band at 1337 cm^{-1} and a ZEKE band at 1266 cm^{-1} – see Figure 8. The assignment that fits in all three electronic states is $14^1 18^1 29^1$ (Table 3). Further, exciting at the position of the weak band at 1034 cm^{-1} gives rise to an emission at 1320 cm^{-1} and a ZEKE band at 1336 cm^{-1}; an assignment that fits all three states is that of the REMPI band to $16^1 18^1$. It may be seen in both the ZEKE spectrum and the 2D-LIF image that there is evidence of weak mixing between the $14^1 18^1 29^1$ and $16^1 18^1$ levels, which is not unexpected, since these levels are of the same symmetry and $\Delta v = 3$ apart – see Figure 7. Also seen in this ZEKE spectrum is a band at 1423 cm^{-1}, which is a good match in both S_1 and D_0^+ for $^+12^1 20^1 30^1$. In the 2D-LIF spectrum in Figure 8, a weak emission can be seen that has a maximum at (1035, 1405) cm^{-1}, also consistent with this assignment. It is unlikely that $12^1 20^1 30^1$ can interact with either $16^1 18^1$ or $14^1 18^1 29^1$, since these would involve $\Delta v = 5$ and $\Delta v = 6$ couplings, respectively. There is, however, a possible coupling to $12^1 14^1 20^2$ which is also expected at about this excitation wavenumber (Table 3), although there is no convincing evidence for this in the ZEKE spectrum (expected at 1557 cm^{-1}), and this was outside the ranges scanned in the 2D-LIF spectra. (Other possible couplings with $11^1 30^2$ or $11^2 20^2$ are both $\Delta v \geq 4$, with some activity in the expected regions of the ZEKE spectrum here, but again the corresponding emissions would be outside scanned regions of the 2D-LIF spectrum.)

4. Other Contributions

With the main assignments detailed above, much of the rest of the 2D-LIF and ZEKE spectra can be assigned as FC activity associated with those levels. However, several are worthy of mention, particularly those that involve vibtor levels. First, the 2D-LIF band at (1018, 1216) cm^{-1} can be associated with the $18^2 20^1 m^4$ level. This assignment to a vibtor level is supported by the appearance of a very weak band at (1018, 218) cm^{-1} (not shown), which may be assigned to $20_1 m_4$ by referring to Table I of Ref. 17; it is also supported by the observation of the weak ZEKE band, $^+20^1 m^4$ (whose wavenumber has been determined previously[16]) when exciting at this wavenumber (Figure 2). The

$^{+}18^{2}20^{1}m^{4}$ ZEKE band is expected at 1176 cm^{-1}, and when exciting at 1019 cm^{-1} a significant new ZEKE band is seen at 1175 cm^{-1} (Figure 2). Since we would not expect the $18^{2}20^{1}m^{4}$ transition to be very intense, we have looked for possible interactions that could be enhancing this. Its overall symmetry is *e*″, which means it could potentially interact with the $m = 1$ levels of totally-symmetric (a_1′) ZOB states, viz. $13^{2}m^{1}$ and $17^{2}m^{1}$, although both of these would involve $\Delta v = 5$ and $\Delta m = 3$, which seems unlikely. Other close-by a_1′ symmetry levels are $11^{1}17^{1}20^{1}$ and $14^{1}18^{1}29^{1}$ (see Table 3) which would each be $\Delta v = 4$ interactions, with the former being the closest energetically; the interaction would also be $\Delta m = 3$, involving the $m = 1$ level of those combinations. Slightly higher is $16^{1}18^{1}$, which would permit a $\Delta v = 3$ (and $\Delta m = 3$, with its $m = 1$ level) interaction, but this seems too distant, and although the levels could have moved as a result of any interaction, the predicted position of 1035 cm^{-1} (Table 3) suggests this is not a likely explanation. Thus, there are pathways for $18^{2}20^{1}m^{4}$ to interact, but these are expected to weaker than the main interactions noted herein. Such couplings would, however, open up further routes for energy flow among the *e*″ levels, including coupling to *e*″ vibtor levels that arise from a_2′ symmetry vibrational levels.

In Refs. 17 and 21, the interaction of $14^{1}m^{6(-)}$ and 14^{2} was discussed. Since $14^{2}30^{2}$ activity is clearly demonstrated in both the ZEKE and 2D-LIF spectra, we might also expect to see $14^{1}30^{2}m^{6(-)}$ activity. The $\Delta(v, m) = 0$ emission band would be expected at 1229 cm^{-1}, and indeed a 2D-LIF band (unlabelled) is seen at (1013, 1229) cm^{-1}, with the emission extending to higher emission wavenumbers, which would be consistent with a $14^{2}30^{2}\ldots14^{1}30^{2}m^{6(-)}$ interaction, with the 14_230_2 emission profile being consistent with this. Since only $14^{2}m^{0}$ can interact with $14^{1}m^{6(-)}$, and so similarly for the 30^{2} combinations, one might expect a separation of the $m = 0$ and $m = 1$ components of $14^{2}30^{2}$, but the spectra are inconclusive on this point.

Additionally, we may expect combinations of 30^{2}, $17^{1}20^{1}$ and $14^{1}20^{1}30^{1}$ with levels that gave rise to other weak bands reported in Ref. 21, $14_120_1m_4$ and $20_2m_{6(+)}$ and $14_120_2m_x$ ($x = 1$ or 2). Although some weak features are at the expected wavenumbers, these are not definitive; however, it is likely interactions are occurring with these levels to some degree. Finally, we note that in Ref. 18 it was found that one other level was coincident with the three essentially coincident 30^{2}, $17^{1}20^{1}$ and $14^{1}20^{1}30^{1}$ bands, namely $19^{2}20^{1}m^{3(-)}$, but no clear evidence for combinations with this level has been found in the present spectra.

D. 900-1000 cm^{-1} bands

In the vertical trace on the right-hand side of Figure 9, it can be seen that there are up to nine bands in this wavenumber region. We have attempted to record ZEKE spectra from each of the indicated positions, with assignable spectra obtained from six of these. These spectra, linked to the excitation position in the REMPI spectrum, are shown in Figure 9. We have also attempted to record both a 2D-LIF spectrum across this region and DF spectra for each of the bands, but these suffered from both poor signal-to-noise, and interference from *m*FT, which had been used in the apparatus prior to recording these spectra. The latter produced some interference with the *p*FT spectra at particular positions, and although these could be straightforwardly identified from ongoing work on *m*FT, we refrain from presenting these 2D-LIF and DF spectra, and just report on the main *p*FT fluorescence activity and assignments, alongside those of the ZEKE spectra.

First, the two REMPI bands at 932 cm^{-1} and 938 cm^{-1} are in the correct region to be associated with transitions to levels formed from the FR bands at ~800 cm^{-1} (see Figure 1) in combination with the vibtor level $20^1m^{3(-)}$. These assignments are supported by both the ZEKE spectra in Figure 9, which show a clear $^+20^1m^{3(-)}$ band at low wavenumber, and by the appearance of the $20_1m_{3(-)}$ band in the 2D-LIF and DF spectra (not shown). Further, we see the $20_129_2m_{3(-)}$ emission band at 1032 cm^{-1} when exciting via both of these bands, in line with the activity seen when exciting via the $9^1/29^2$ FR pair.[22] In the ZEKE spectrum, we see both strong $^+9^120^1m^{3(-)}$ and $^+20^129^2m^{3(-)}$ bands when exciting via the lower-wavenumber band, but with the latter dominating the spectrum when exciting via the higher-wavenumber band. This behaviour is again consistent with what we saw when exciting via the $9^1/29^2$ FR pair.[22] Together with other expected FC activity, this accounts for the main bands seen in the ZEKE spectra.

Moving onto the next REMPI band at 947 cm^{-1}, this shows a strong ZEKE band at 981 cm^{-1}, with another band at 1276 cm^{-1}. The latter may be assigned to $^+13^118^1$, which suggests that the REMPI band comprises overlapping contributions, with one being the HT active 13^118^1; this is confirmed by a band in the DF spectrum at 1313 cm^{-1}. The other contribution is suggested as being 8^1, giving rise to the most intense ZEKE band $^+8^1$ at 981 cm^{-1}, which would be consistent with the calculated wavenumbers in Table 1 for the S_1 and D_0^+ states; further, the DF shows a strong band at 990 cm^{-1}, which is also reasonably consistent with the calculated and previous experimental values; however, we view the 8^1 assignment as tentative.

The next REMPI band at 952 cm^{-1} gives rise to a ZEKE spectrum with a strong band at 993 cm^{-1}, while the DF shows a strong band at 1062 cm^{-1}, the excitation position and both of these bands are consistent with an assignment of the REMPI band to $28^{1}29^{1}$.

Exciting at the position of the REMPI band at 960 cm^{-1} gives rise to a strong ZEKE band at 1012 cm^{-1}, while the DF yields a strong band at 1091 cm^{-1}; the excitation position and both of these bands support the assignment of the REMPI band to the HT-active $11^{1}28^{1}$ transition.

No satisfactory ZEKE spectra were obtained from the bands at 968 cm^{-1} and 975 cm^{-1}, but we did see a weak $20_1 m_4$ emission band when exciting via the latter band. Tentatively, we therefore assign these two bands to the $9^{1}/29^{2}$ FR pair, each in combination with $20^{1}m^{4}$.

The band at 984 cm^{-1} may be satisfactorily assigned to $18^{2}20^{1}m^{3(-)}$ from the ZEKE spectrum, which shows a strong band at 1141 cm^{-1}, which can be assigned to $^{+}18^{2}20^{1}m^{3(-)}$. No satisfactory DF spectrum was obtained from this feature. Finally, although a very weak ZEKE spectrum was obtained at the position of the 992 cm^{-1} REMPI band, its assignment is unclear and so it is not shown; it may arise from overlapped excitation levels.

IV. CONCLUDING REMARKS

In this work, an apparently simple, albeit broadened, feature in the REMPI spectrum has been found to consist of at least ten and likely more transitions, even at only ~1000 cm^{-1} internal energy. Further, many of these involve S_1 vibrational eigenstates that arise from the interaction of a number of ZOSs. This complexity, owing to interactions occurring via a growing bath of vibrational and vibtor levels, is implied in the broadness of the overall spectral activity in the central region of the ZEKE spectra (Figure 3) and the wealth of activity in the 2D-LIF spectrum (Figure 4). In our previous work,[13,16,18,19,20,21,22] and that of the Lawrance group,[17] a large number of torsional, vibtor and vibrational levels have been assigned in the S_0, S_1 and D_0^+ states of *p*FT. From these, reliable gas-phase values of the fundamental vibrational wavenumbers (excluding methyl-localized ones) have been obtained (Table 1). As a consequence, detailed and robust assignments of the ZEKE and 2D-LIF spectra can be obtained, and this is particularly important in allowing overlapped and interacting levels in the S_1 state to be identified. By so doing, we have deduced that the two ZOB states, 13^{2} and 17^{2}, give rise to the main intensity here, and have also established the main interactions with these, which are summarized in

Figure 7. These are mostly Δv = 3 interactions, which are expected to be the strongest type of anharmonic interaction. Although the levels studied lie at only 1000 cm^{-1}, Figure 7 shows the highly-linked nature of the interactions, and the build-up in complexity. So if, for example, a photophysical or collisional process led to the deposition of energy into the 13^2 levels, then we can see that, in a time-resolved picture, a rapid redistribution of energy would occur to other vibrational and torsional motions. Thus, the initially well-defined motion of the molecule would rapidly become highly chaotic, making reliable predictions of reactivity/dissociation behaviour much more complicated. This phenomenon would clearly become more pronounced at higher internal energies.

We have only discussed these interactions qualitatively, since there are a number of such interactions and obtaining enough reliable intensity data is not feasible; this is especially the case, since the Franck-Condon factors for the different transitions appear to be quite complicated, as we saw for the $9^1 \ldots 29^2$ interaction discussed in Ref. 22. These comments also apply to attempting to compare explicitly calculated anharmonicity corrections with quantum chemical methods, where the accuracy in the calculated harmonic vibrational wavenumbers is not good enough to merit the large additional computational cost –this is particularly the case for the S_1 state (see previous papers from our group, and refer to Table 1).

The appearance of both the ZEKE and 2D-LIF spectra support the following picture. The 13^2 and 17^2 ZOB states are, essentially independently, strongly coupling to nearby levels of the same symmetry, and that then further couplings occur, as indicated in Figure 7. In the "tier model" of IVR,[1] the ZOSs directly coupled to the two main ZOB states could be termed "doorway states", then the subsequent Δv = 3 couplings are key to opening up routes into the growing bath of background levels. It is notable that the $15^1 20^3$ state does not interact with either ZOB state, owing to the large Δv coupling required. Slightly higher in wavenumber, the $16^1 18^1$ state is present and also undergoes coupling. We have also suggested a different route for energy flow among a_1'' symmetry levels. Consequently, in a time-dependent picture, there are multiple routes for energy to flow through the *p*FT molecule and these provide different routes to coupling with the bath of levels.

We have noted that m = 1 vibtor levels of a_1' vibrations can couple with other vibtor levels of e'' symmetry, and this would also include those involving vibrational levels of a_2' symmetry. Further, the m = 1 vibtor levels of the HT-active a_1'' levels can interact with other vibtor levels of e' symmetry, including those involving vibrations of a_2'' symmetry. Although we do not see explicit bands associated with these further couplings, our observation of such in previous work makes it likely these are present

– thus, there would likely be routes for energy to flow through vibrational levels of any symmetry. We also propose other couplings, including those involving vibtor levels with $m \neq 0$ or 1, with levels involving 20^1m^4 apparently being the most significant, involving other vibrational levels. Evidence for interactions with other vibtor levels is present, but seems to be higher order and so weaker. Over longer experimental timescales, and/or with higher resolution, the involvement of other levels from the bath states is expected to be more evident. Together, these couplings lead to the wealth of structure and the broad "background" signals seen in the ZEKE and 2D-LIF spectra, but in the REMPI spectrum, these are all contained underneath the 1013 cm^{-1} band.

We have been able to extract a large amount of information from the spectra recorded here, allowing the key steps in the IVR process to be elucidated. What is surprising is that even at only ~1000 cm^{-1} internal excitation, multiple, overlapping, but essentially independent, routes to energy flow have been identified. Clearly, vibrational combinations involving the 13^2 and 17^2 ZOB states will appear at higher wavenumbers and be involved in more extensive couplings. Thus, it is straightforward to see how a rapid, statistical, dispersal of internal energy amongst the vibrational and torsional (and rotational) motions will occur at larger excitation energies. The results here show that there will, however, be different routes for energy flow and it is likely that will have different efficiencies.

Acknowledgements

We are grateful to the EPSRC for funding (grant EP/L021366/1). The EPSRC and the University of Nottingham are thanked for studentships to L.E.W, D.J.K. and W.D.T. We are grateful to Lewis Warner who helped to record some DF spectra as part of an Undergraduate Summer Bursary project funded via a University of Nottingham School of Chemistry 1960 scholarship. We are grateful for ongoing discussions with Warren Lawrance and Jason Gascooke (Flinders, Adelaide).

Table 1: Calculated and experimental wavenumbers for the vibrations of *p*FT in the three electronic states of interest.

D_i	S_0		S_1		D_0^+	
	Calculated[a]	Experiment[b]	Calculated[a]	Experiment[c]	Calculated[a]	Experiment[d]
			a_1'			
1	3103	3068	3130		3116	
2	3071	3068	3105		3101	
3	1598	1603[e]	1528		1628	1631
4	1499	1513	1432		1454	
5	1209	1241[e]	1213	1230	1311	1338
6	1192	1215[e]	1185	1194	1211	1234
7	1145	1159[e]	1120		1158	1170
8	1005	982[e]	954	947	969	981
9	827	843[f]	805	797	811	824
10	715	730[e]	700	711	710	721
11	446	453[f]	410	408	437	440
			a_2'			
12	953	950[e]	588	618	987	985
13	808	814[e]	484	512	770	777
14	418	414[f]	172	199	356	350
			a_2''			
15	931	925[e]	706	687	998	1004
16	817	819[e]	651	609	832	842
17	698	697[e]	538	509	671	685
18	500	500[e]	468	426	488	499
19	330	334[f]	243	239	266	271
20	141	143[f]	110	104	109	111
			a_1''			
21	3102	3040	3126		3115	
22	3071	3040	3100		3101	
23	1586	1592	1427		1383	
24	1395	1435	1315		1470	
25	1283	1300	935		1301	
26	1292	1321	1255		1250	
27	1090	1099	1053		1115	
28	633	640[f]	546	552	564	570
29	414	424[f]	395	399	412	416
30	298	307[f]	307	309	313	320

[a] Calculated wavenumbers have been presented in our previous work.[16,18,21,22] The level of theory employed is B3LYP/aug-cc-pVTZ for the S_0 state; TD-B3LYP/aug-cc-pVTZ for the S_1 state, and UB3LYP/aug-cc-pVTZ for the D_0^+ state (where spin contamination was minimal). In all cases, the calculated harmonic wavenumbers have been scaled by 0.97.

[b] For the S_0 state, unless indicated otherwise, the tabulated values are those recommended in Ref. 40, originating from IR and Raman studies. Many of these have now been superseded by gas-phase values recorded from 2D-LIF studies on jet-cooled samples, as indicated.

[c] These values are those obtained from 2D-LIF, LIF and REMPI studies on jet-cooled samples. [16,17,18,21,22] The lowest-wavenumber a_2' and a_2'' symmetry vibrations were obtained after taking into account vibtor interactions.[17] The value for D_8 is tentative – see text. Several values have undergone revision between studies: those included here are the most recent.

[d] These values are those obtained from ZEKE studies on jet-cooled samples from our previous work.[16,18,21,22] Several values have undergone revision between studies: those included here are the most recent, with the values sometimes being our best estimate from combination bands observed via different intermediate levels, and sometimes with differing band shapes.

[e] These values were determined from 2D-LIF studies by our group – see Refs. 21, 22, and 47. The value for D_8 is tentative – see text.

[f] These values were determined from 2D-LIF studies by Lawrance and coworkers.[17] The lowest-wavenumber a_2' and a_2'' symmetry vibrations were obtained after taking into account vibtor interactions. The perturbed values of the latter, and the wavenumbers of other vibrations reported in our work, [21,22,47] are consistent with those reported in Ref. 17.

Table 2: Correspondence of the C_{2v} point group symmetry classes with those of the G_{12} molecular symmetry group. Also indicated are the symmetries of the D_i vibrations and the different pure torsional levels.[a]

C_{2v}	G_{12}	D_i [b]	m
a_1	a_1'	D_1–D_{11}	0, 6(+)
a_2	a_2'	D_{12}–D_{14}	6(-)
b_1	a_2''	D_{15}–D_{20}	3(-)
b_2	a_1''	D_{20}–D_{30}	3(+)
	e'		2,4
	e''		1,5

[a] Symmetries of vibtor levels can be obtained by combining the vibrational symmetry (in G_{12}) with those of the pure torsional level, using the D_{3h} point group direct product table.

[b] The D_i labels are described in Ref. 40, where the vibrational mode diagrams can also be found.

Table 3 FC and HT-allowed vibrational combinations that could be contributing to the 1013 cm^{-1} feature

Level	Symmetry	S_1	S_0	D_0^+
$18^1 19^2 20^1$	a_1'	1008	1311	1152
$15^1 20^3$	a_1'	1011[a]	1354	1337
$14^2 17^1 20^1$	a_1'	1011	1668	1496
$14^1 20^1 29^1 30^1$	a_1''	1011	1288	1197
$17^1 20^1 29^1$	a_1''	1012	1264	1212
$10^1 14^1 20^1$	a_1''	1014	1287	1182
$13^1 14^2 20^1$	a_1''	1014	1785	1588
$13^1 20^1 29^1$	a_1'	1015	1381	1304
$11^1 20^2 29^1$	a_1''	1015	1163	1078
$14^2 30^2$	a_1'	1016	1442	1340
$14^1 16^1 20^2$	a_1''	1016	1519	1414
$14^3 20^1 30^1$	a_1'	1016[b]	1692	1481
$14^1 17^1 30^1$	a_1'	1017	1418	1355
$9^1 20^2$	a_1'	1017[a]	1129	1046
$29^1 30^2$	a_1''	1017	1038	1056
17^2	a_1'	1018	1394	1370
$20^2 29^2$	a_1'	1018[a]	1134	1054
$10^1 30^1$	a_1''	1020	1037	1041
$13^1 14^1 30^1$	a_1''	1020	1535	1447
$11^1 14^1 20^1 30^1$	a_1'	1020	1317	1221
$13^1 17^1$	a_1''	1021	1511	1462
$11^1 17^1 20^1$	a_1'	1021	1293	1236
$16^1 20^1 30^1$	a_1''	1022	1269	1273
$14^3 18^1$	a_1''	1023	1742	1549
13^2	a_1'	1024	1628	1554
$14^1 18^1 29^1$	a_1'	1024	1338	1265
$11^1 13^1 20^1$	a_1''	1024	1410	1328
$11^1 30^2$	a_1'	1026	1067	1080
$12^1 20^1 30^1$	a_1'	1031	1400	1416
$11^1 14^1 18^1$	a_1''	1033	1367	1289
$16^1 18^1$	a_1'	1035	1319	1341
$11^2 20^2$	a_1'	1036[a]	1192	1102
$12^1 14^1 20^2$	a_1'	1037[a]	1650	1557

[a] For combinations in S_1 that involve 20^2, the value of 220 cm^{-1} was employed for this component, the experimental wavenumber for this overtone, [17] rather than 2×104 cm^{-1}.

[b] For $14^320^130^1$, the experimental wavenumber for $14^120^130^1$ (Ref. 18) was used in deducing the wavenumber in S_1.

Figure Captions

Figure 1: Long REMPI scan (0 – 1250 cm^{-1}), with limited labelling showing the torsional region and the 400 cm^{-1}, 800 cm^{-1}, 845 cm^{-1}, 1013 cm^{-1} and 1200 cm^{-1} regions. The insert shows an expanded view of the REMPI spectrum in the range 920–1050 cm^{-1}, and is the focus of the present work.

Figure 2: ZEKE spectra (0–2000 cm^{-1}) recorded across the 1013 cm^{-1} band. The 1013 cm^{-1} REMPI band is shown as a vertical trace on the right-hand side of the figure, with the excitation positions indicated, and linked to the relevant ZEKE spectra. An expansion of the central region of the ZEKE spectra is shown in Figure 3.The preceding superscripted + signs used in the text on assignments have been omitted for clarity.

Figure 3: Expanded view of the central region (900–1700 cm^{-1}) of a selection of the ZEKE spectra shown in Figure 2. The main part of the 1013 cm^{-1} REMPI band is shown as a vertical trace on the right-hand side of the figure, with the excitation positions indicated, and linked to the relevant ZEKE spectra. Assignments indicated in the same (non-black) colour are the main interacting levels discussed in the text – see also Figure 7. The preceding superscripted + signs used in the text on assignments have been omitted for clarity.

Figure 4: Overview 2D-LIF spectrum across the main 1013 cm^{-1} band. The main contributing states to the emission are indicated at the top of the spectrum. To the right of the spectrum is a trace of the fluorescence intensity integrated across the image. Some of the key bands are labelled – see text for further discussion. An expanded view of the higher-wavenumber region is shown in Figure 5. Assignments indicated in the same (non-black) colour are the main interacting levels discussed in the text – see also Figure 7.

Figure 5: Expanded view of the section of the 2D-LIF spectrum in Figure 4 recorded across the 1013 cm^{-1} band showing the key activity associated with the main interacting levels. To the immediate right of the spectrum is a trace of the fluorescence intensity integrated across the image. Some of the key bands are labelled. To the far right of the figure, plots of the intensity variation of some key bands are presented. See text for further discussion. Assignments indicated in the same (non-black) colour are the main interacting levels discussed in the text – see also Figure 7.

Figure 6: Schematic showing the main 1013 cm^{-1} REMPI band, and indications of other expected combination band activity. (a) The 1013 cm^{-1} REMPI band; (b) the bands at ~400 cm^{-1} studied in Ref. 21, shifted by an amount corresponding to the overlapped features 30^2, 17^120^1 and $14^120^130^1$; and (c) the bands at ~800 cm^{-1} studied in Ref. 22 shifted by an amount corresponding to 20^2.

Figure 7: Schematic showing the main couplings between the ZOB states and other levels. Assignments indicated in the same colour are the main interacting levels discussed in the text, and correspond to those in Figures 3–5. The results of these interactions are a set of vibrational eigenstates of the S_1 electronic state that given rise to the main 1013 cm^{-1} REMPI band in Figure 1. There will be corresponding, but separate, eigenstates involving m = 0 and m = 1 levels. The majority of the intensity is from the top two sets of levels. Three of the sets of m= 0 levels have a_1' symmetry, and one has a_1'' symmetry. See text for further discussion.

Figure 8: Spectra recorded at wavenumbers corresponding to the two bands in the range $S_1 0^0$ + 1020–1040 cm^{-1} (see Figure 1). (a) 2D-LIF spectrum; (b) ZEKE spectra. Assignments are discussed in the text.

Figure 9: ZEKE spectra recorded via the weak 900–1000 cm^{-1} features. On the right-hand side, the relevant section of the REMPI spectrum is shown, with the excitation positions indicated; these are linked to the appropriate ZEKE spectra.

Figure 1

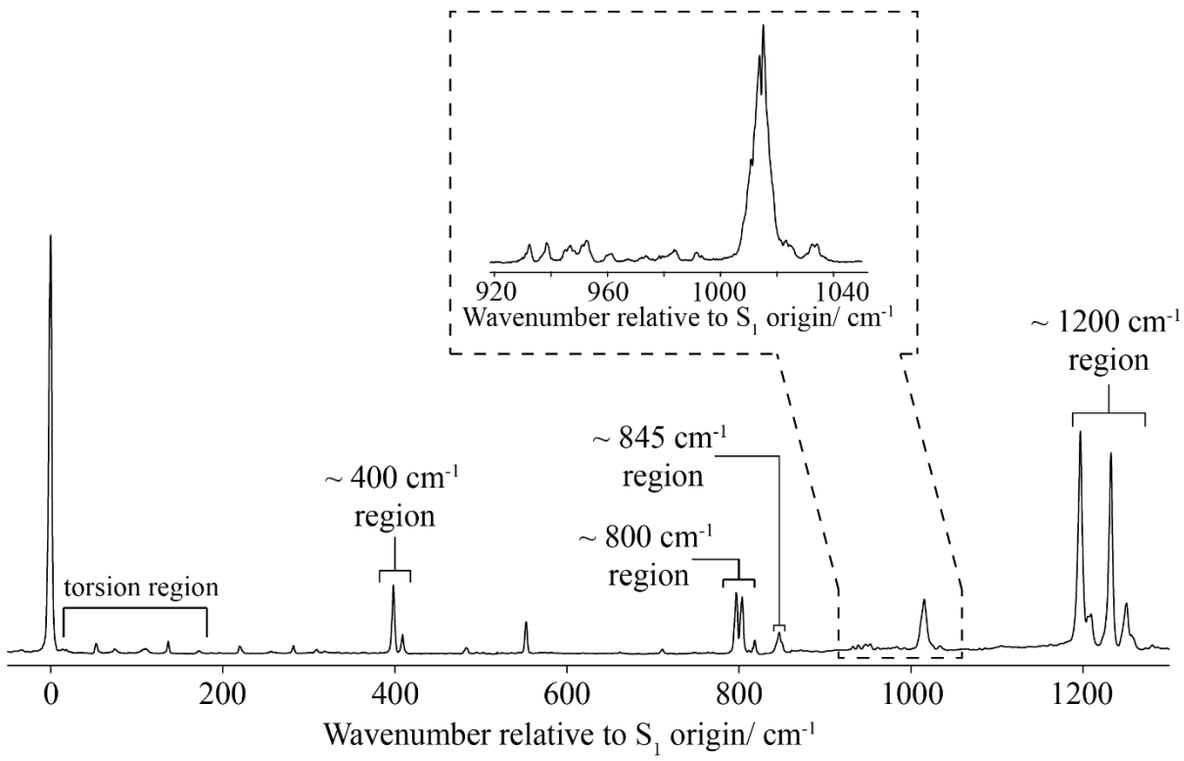

Figure 2

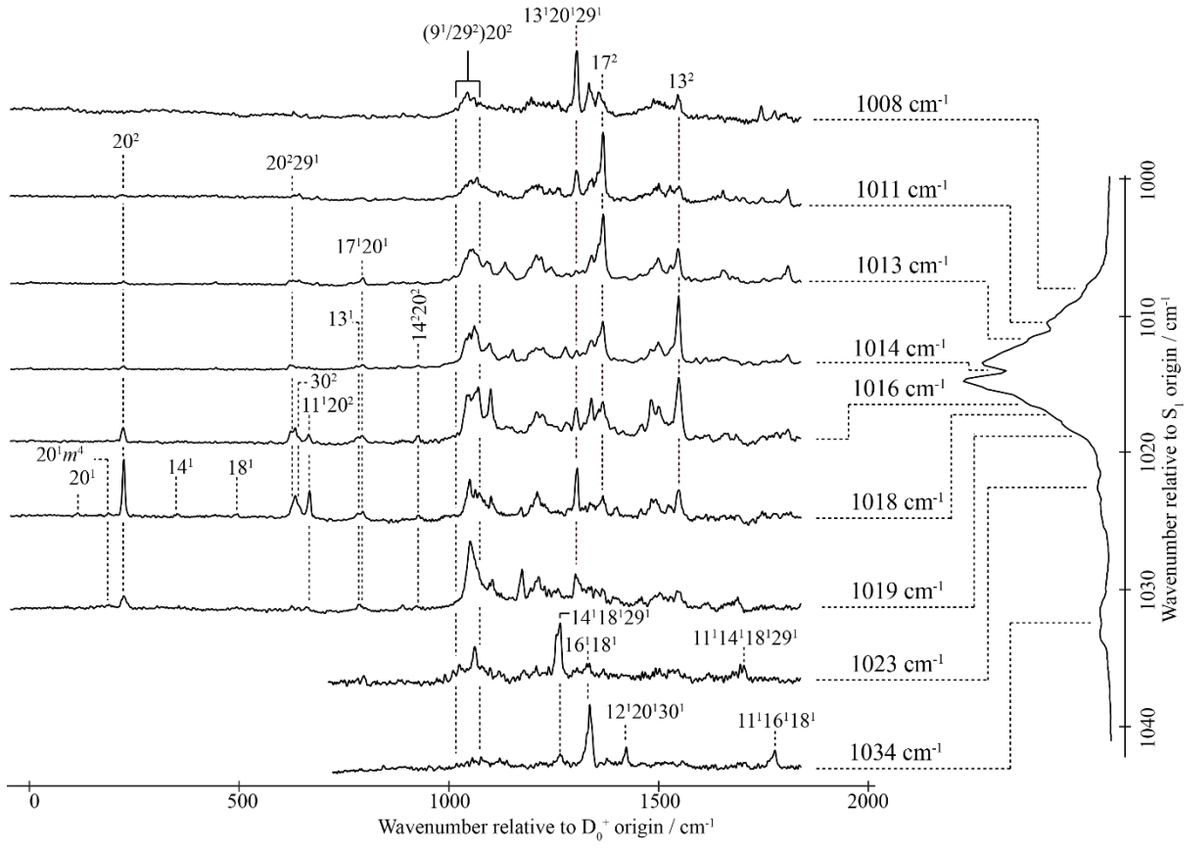

Figure 3

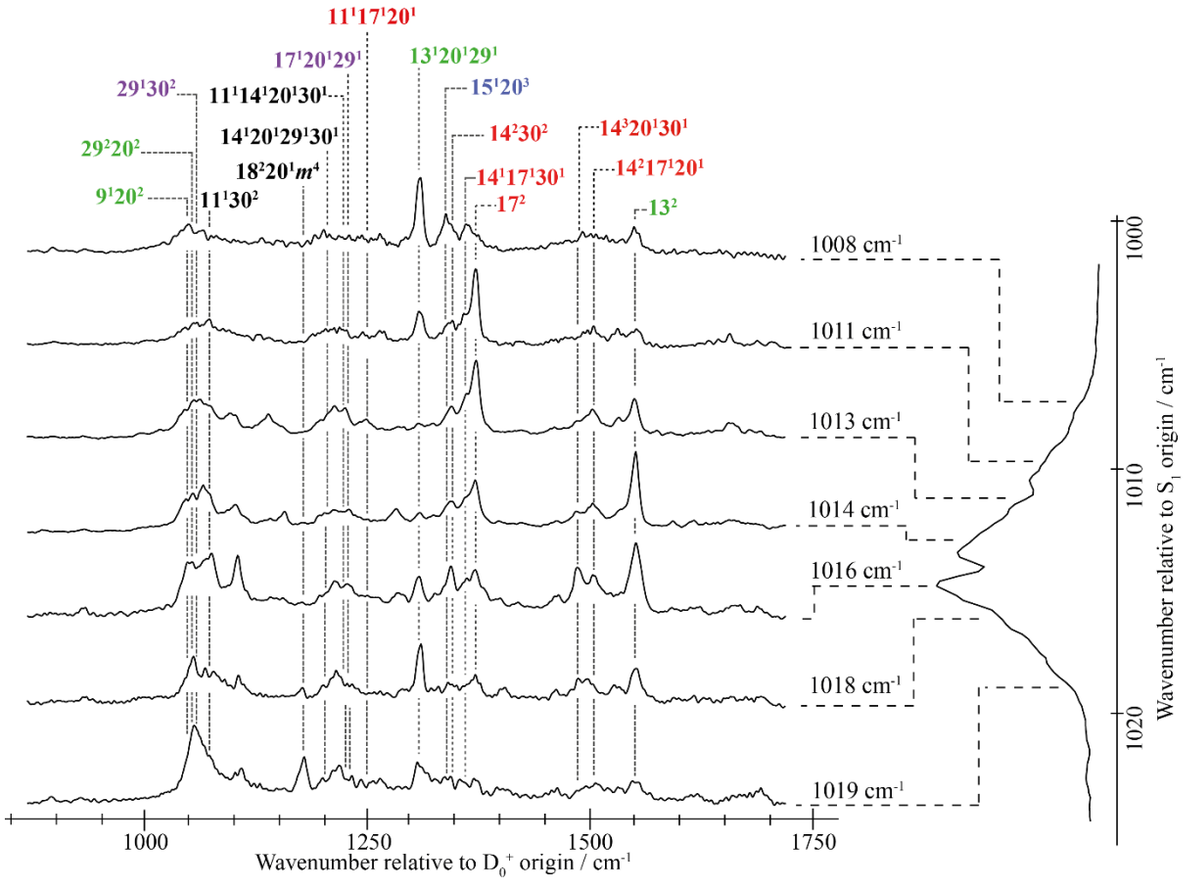

Figure 4

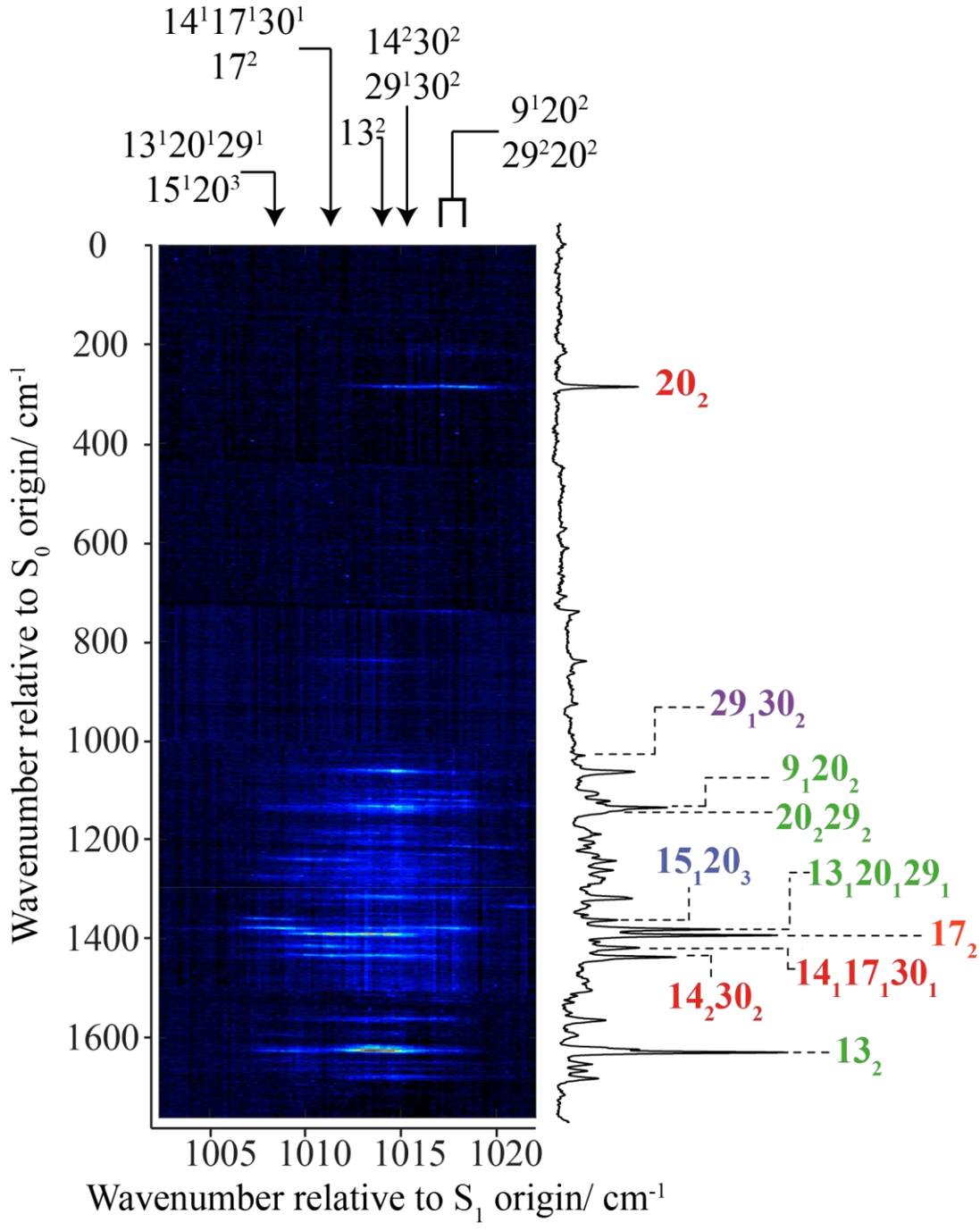

Figure 5

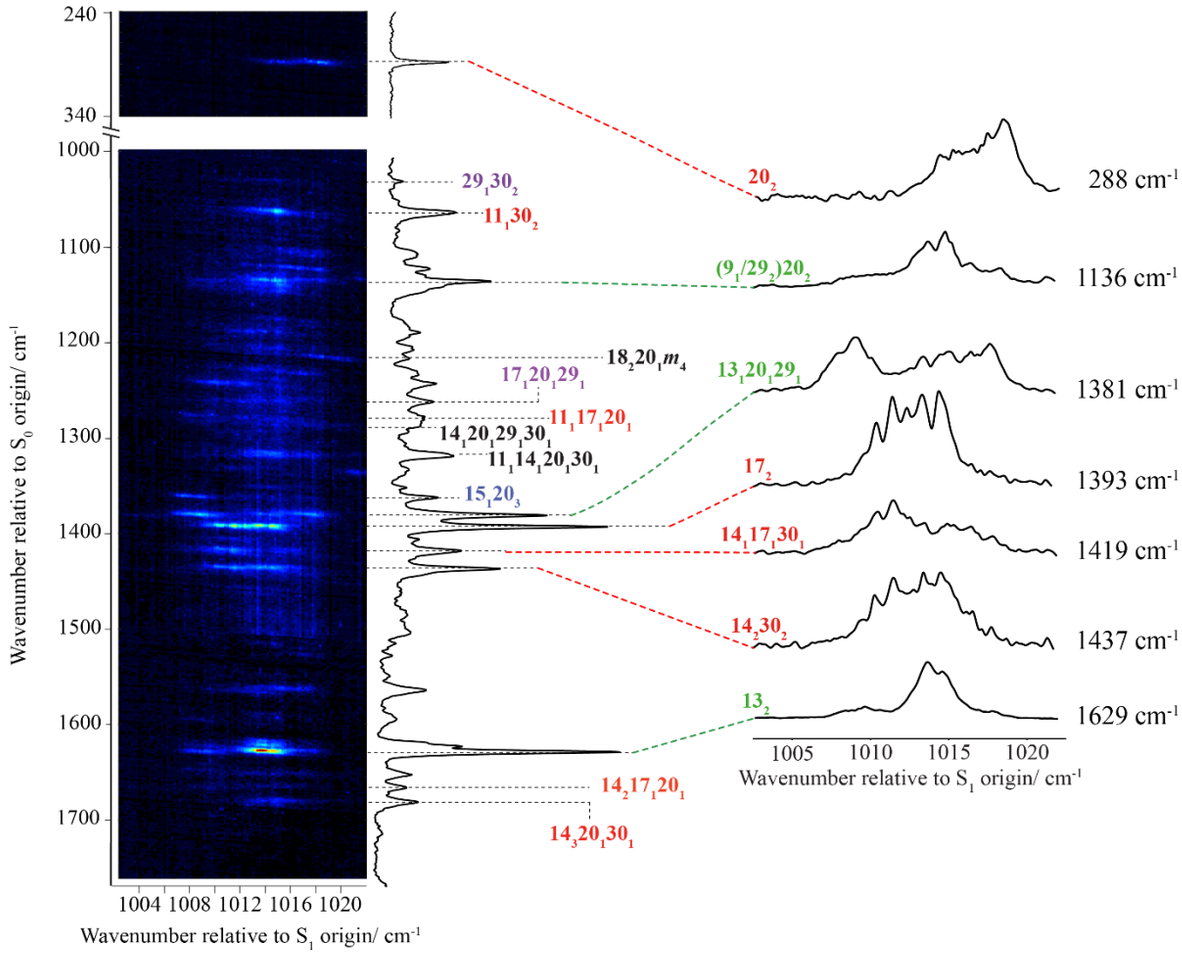

Figure 6

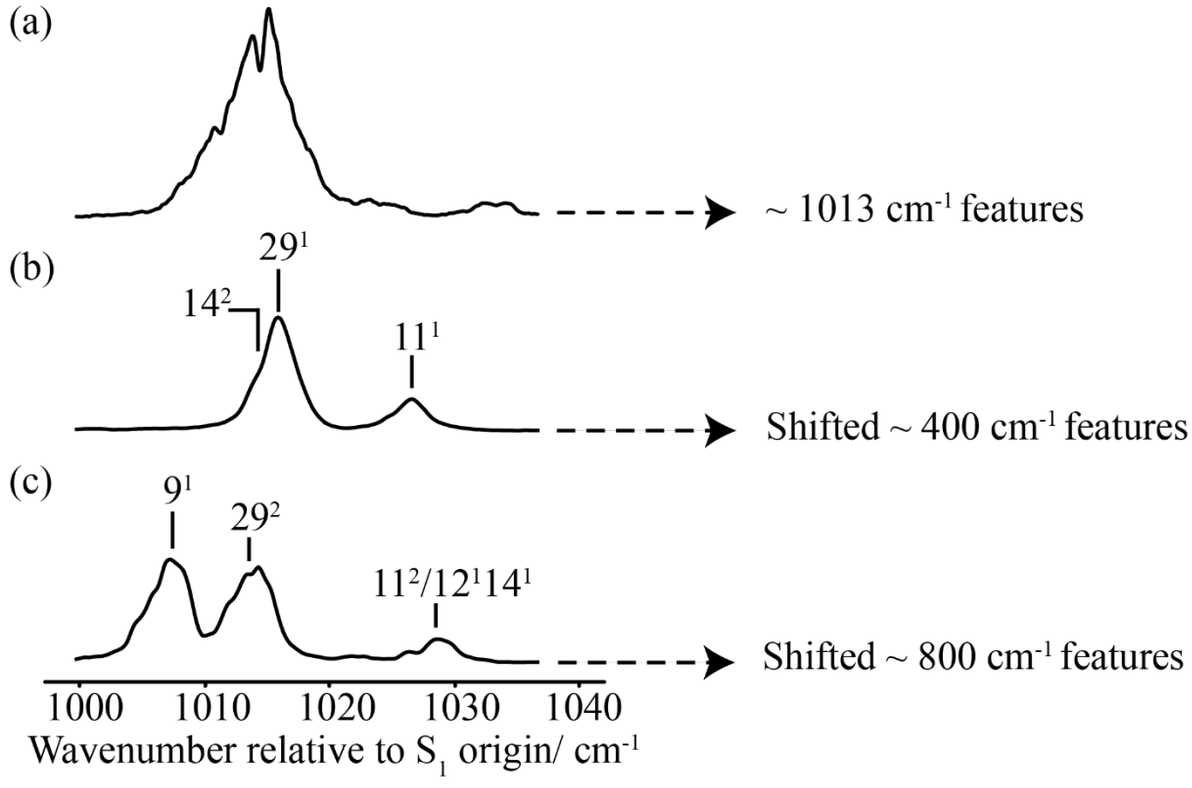

Figure 7

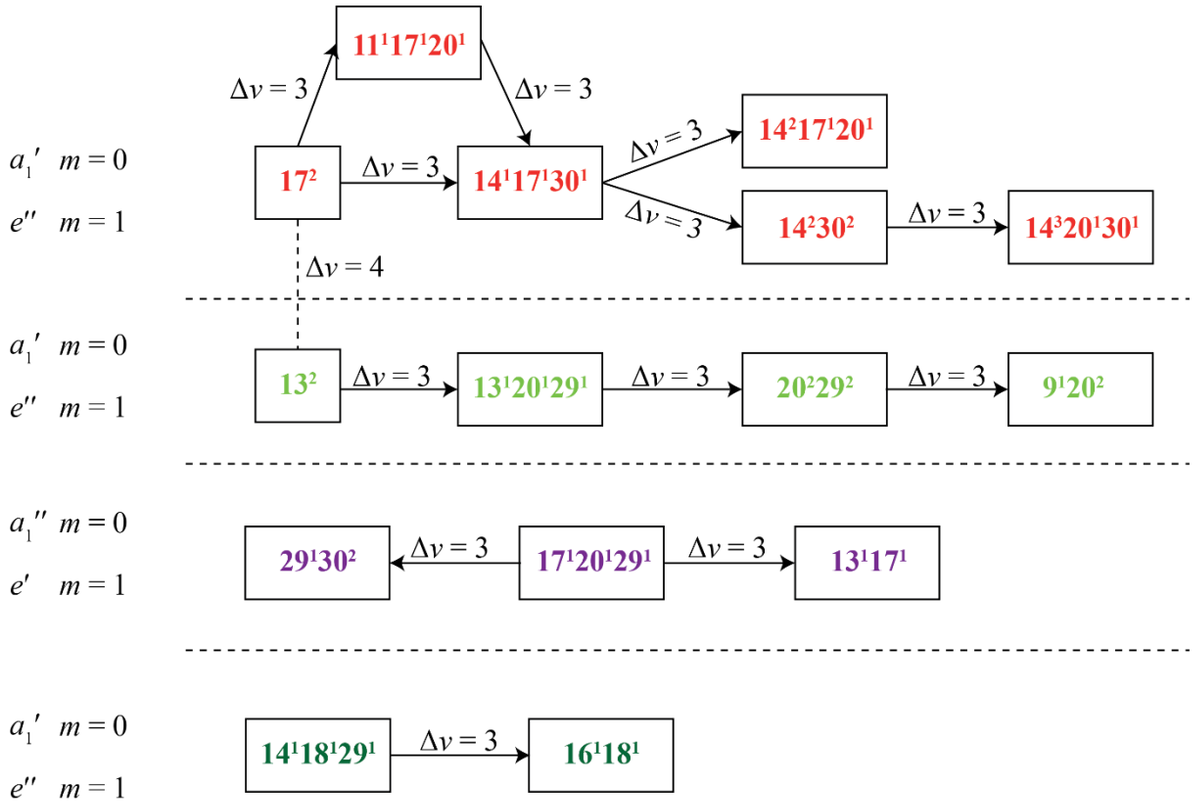

Figure 8

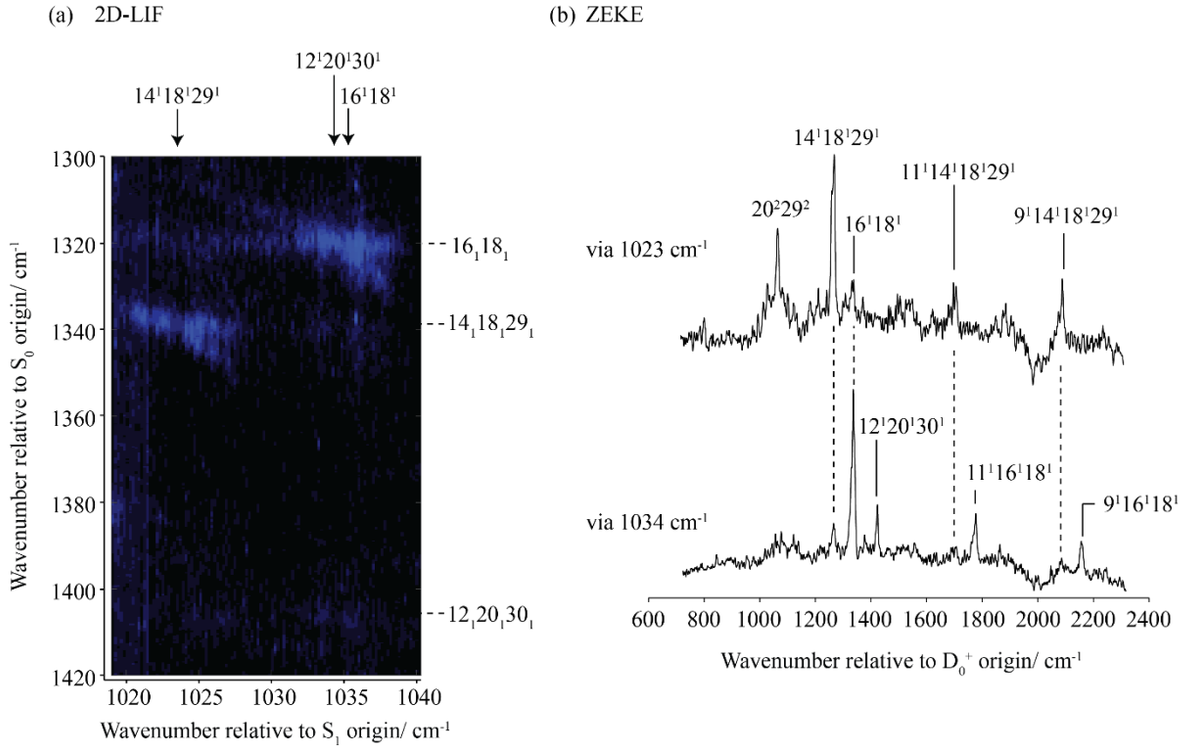

Figure 9

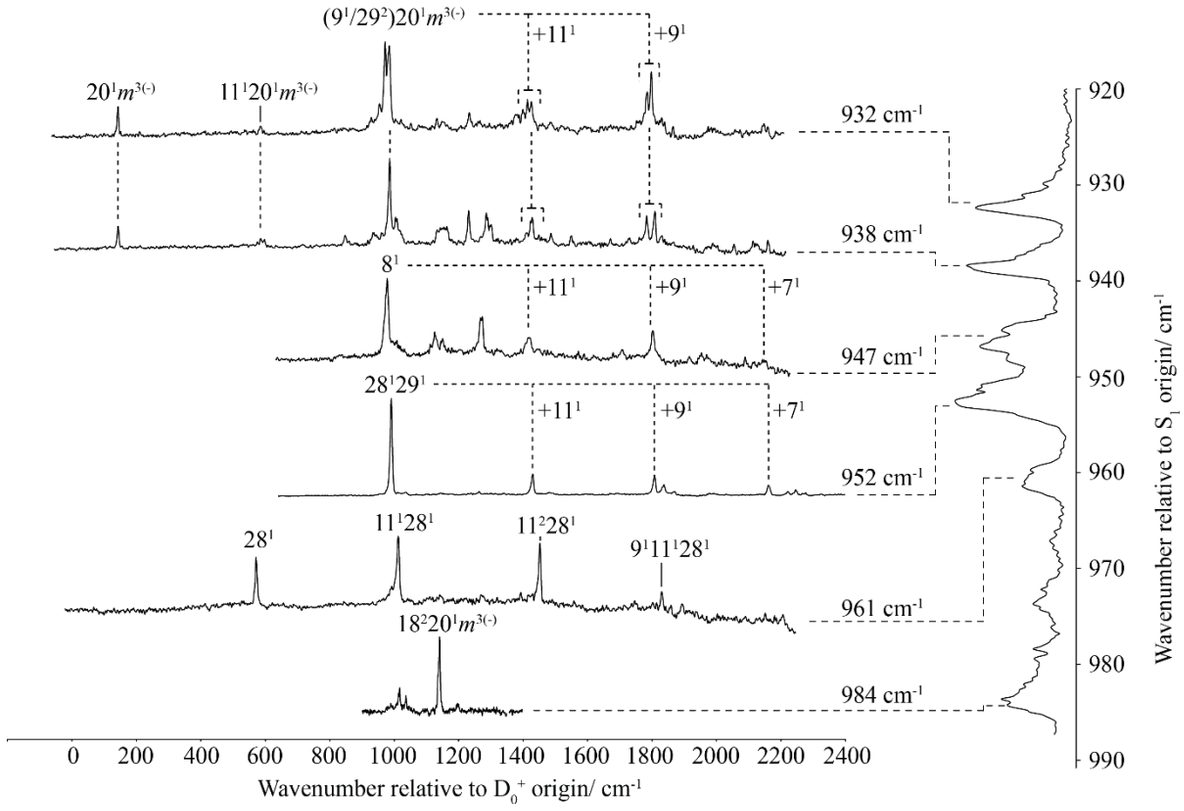

References

[1] D. J. Nesbitt and R. W. Field, J. Phys. Chem. **100**, 12735 (1996).

[2] C. S. Parmenter and B. M. Stone, J. Chem. Phys. **84**, 4710 (1986).

[3] D. B. Moss and C. S. Parmenter, J. Chem. Phys. **98**, 6897 (1993).

[4] Z.-Q. Zhao and C. S. Parmenter, *Mode Selective Chemistry* (Kluwer, 1991) Eds. J. Jortner, R. D. Levine, and B. Pullman. Jerusalem Symp. Quant. Chem. Biochem. **24**, 127 (1991).

[5] Z.-Q. Zhao, C. S. Parmenter, D. B. Moss, A. J. Bradley, A. E. W. Knight, and K. G. Owens, J. Chem. Phys. **96**, 6362 (1992).

[6] Z.-Q. Zhao, PhD Thesis, Indiana University (1992).

[7] P. J. Timbers, C. S. Parmenter, and D. B Moss, J. Chem. Phys. **100**, 1028 (1994).

[8] Q. Ju, C. S. Parmenter, T. A. Stone, and Z.-Q. Zhao, Isr. J. Chem. **37**, 379 (1997).

[9] W. T. Cave and H. W. Thompson, Faraday Soc. Trans. **9**, 35 (1950).

[10] T. Cvitaš and J. M. Hollas, Molec. Phys., **20**, 645 (1971).

[11] C. J. Seliskar, M. A. Leugers, M. Heaven, and J. L. Hardwick, J. Molec. Spect. **106**, 330 (1984).

[12] K. Okuyama, N. Mikami, and M. Ito, J. Phys. Chem. **89**, 5617 (1985).

[13] V. L. Ayles, C. J. Hammond, D. E. Bergeron, O. J. Richards, and T. G. Wright, J. Chem. Phys. **126**, 244304 (2007).

[14] C. J. Hammond, V. L. Ayles, D. E. Bergeron, K. L. Reid, and T. G. Wright, J. Chem. Phys. **125**, 124308 (2006).

[15] J. A. Davies, A. M. Green, A. M. Gardner, C. D. Withers, and T. G. Wright, Phys. Chem. Chem. Phys. **16**, 430 (2014).

[16] A. M. Gardner, W. D. Tuttle, L. Whalley, A. Claydon, J. H. Carter, and T. G. Wright, J. Chem. Phys. **145**, 124307 (2016).

[17] J. R. Gascooke, L. D. Stewart, P. G. Sibley, and W. D. Lawrance, J. Chem. Phys. **149**, 074301 (2018).

[18] W. D. Tuttle, A. M. Gardner, L. E. Whalley, and T. G. Wright, J. Chem. Phys. **146**, 244310 (2017).

[19] A. M. Gardner, W. D. Tuttle, L. E. Whalley, and T. G. Wright, Chem. Sci. **9**, 2270 (2018).

[20] W. D. Tuttle, A. M. Gardner, L. E. Whalley, D. J. Kemp, and T. G. Wright, Phys. Chem. Chem. Phys. **21**, 14133 (2019).

[21] D. J. Kemp, A. M. Gardner, W. D. Tuttle, and T. G. Wright, Molec. Phys. (2019) In press. https://doi.org/10.1080/00268976.2018.1554865

[22] D. J. Kemp, L. E. Whalley, A. M. Gardner, W. D. Tuttle, L. G. Warner, and T. G. Wright, J. Chem. Phys. **150**, 064306 (2019).

[23] A. M. Gardner, A. M. Green, V. M. Tamé-Reyes, K. L. Reid, J. A. Davies, V. H. K. Parkes, and T. G. Wright, J. Chem. Phys. **140**, 114308 (2014).

[24] A. M. Gardner, A. M. Green, V. M. Tamé-Reyes, V. H. K. Wilton, and T. G. Wright, J. Chem. Phys. **138**, 134303 (2013).

[25] E. A. Virgo, J. R. Gascooke, and W. D. Lawrance, J. Chem. Phys. **140**, 154310 (2014).

[26] J. R. Gascooke, E. A. Virgo, and W. D. Lawrance, J. Chem. Phys. **142**, 024315 (2015).

[27] J. R. Gascooke, E. A. Virgo, and W. D. Lawrance, J. Chem. Phys. **143**, 044313 (2015).

[28] J. R. Gascooke and W. D. Lawrance, J. Molec. Spec., **318**, 53 (2015).

[29] A. M. Gardner, W. D. Tuttle, P. Groner, and T. G. Wright, J. Chem. Phys. **146**, 124308 (2017).

[30] W. D. Tuttle, A. M. Gardner, K. B. O'Regan, W. Malewicz, and T. G. Wright, J. Chem. Phys. **146**, 124309 (2017).

[31] L. D. Stewart, J. R. Gascooke, and W. D. Lawrance, J. Chem. Phys. **150**, 174303 (2019).

[32] D. J. Kemp, E. F. Fryer, A. R. Davies, and T. G. Wright, J. Chem. Phys. **151**, 084311 (2019).

[33] N. J. Reilly, T. W. Schmidt, and S. H. Kable, J. Phys. Chem. A **110**, 12355 (2006).

[34] J. R. Gascooke and W. D. Lawrance, Eur. Phys. J. D **71**, 287 (2017).

[35] E. B. Wilson, Jr, Phys. Rev., **45**, 706 (1934).

[36] G. Varsányi, *Assignments of the Vibrational Spectra of Seven Hundred Benzene Derivatives*, Wiley, New York, 1974.

[37] R. S. Mulliken, J. Chem. Phys., **23**, 1997 (1955).

[38] G. Herzberg, *Molecular Spectra and Molecular Structure II. Infrared and Raman Spectra of Polyatomic Molecules*, Krieger, Malabar, 1991.

[39] A. M. Gardner and T. G. Wright, J. Chem. Phys., **135**, 114305 (2011).

[40] A. Andrejeva, A. M. Gardner, W. D. Tuttle, and T. G. Wright, J. Molec. Spect. **321**, 28 (2016).

[41] P. J. Breen, J. A. Warren, E. R. Bernstein, and J. I. Seeman, J. Chem. Phys. **87**, 1917 (1987).

[42] E. Fermi, Z. Phys., **71**, 250 (1931).

[43] J. R. Gascooke and W. D. Lawrance, J. Chem. Phys. **138**, 134302 (2013).

[44] N. T. Whetton and W. D. Lawrance, J. Phys. Chem. **93**, 5377 (1989).

[45] Z.-Q. Zhao and C. S. Parmenter, Ber. Bunsenges. Phys. Chem. **99**, 536 (1995).

[46] J. A. Davies and K. L. Reid, Phys. Rev. Lett. **109**, 193004 (2012).

[47] D. J. Kemp, W. D. Tuttle, A. M. Gardner, L. E. Whalley, and T. G. Wright, J. Chem. Phys. **151**, 064308 (2019).

[48] B. T. Darling and D. M. Dennison, Phys. Rev. **57**, 128 (1940).

The Journal of Chemical Physics

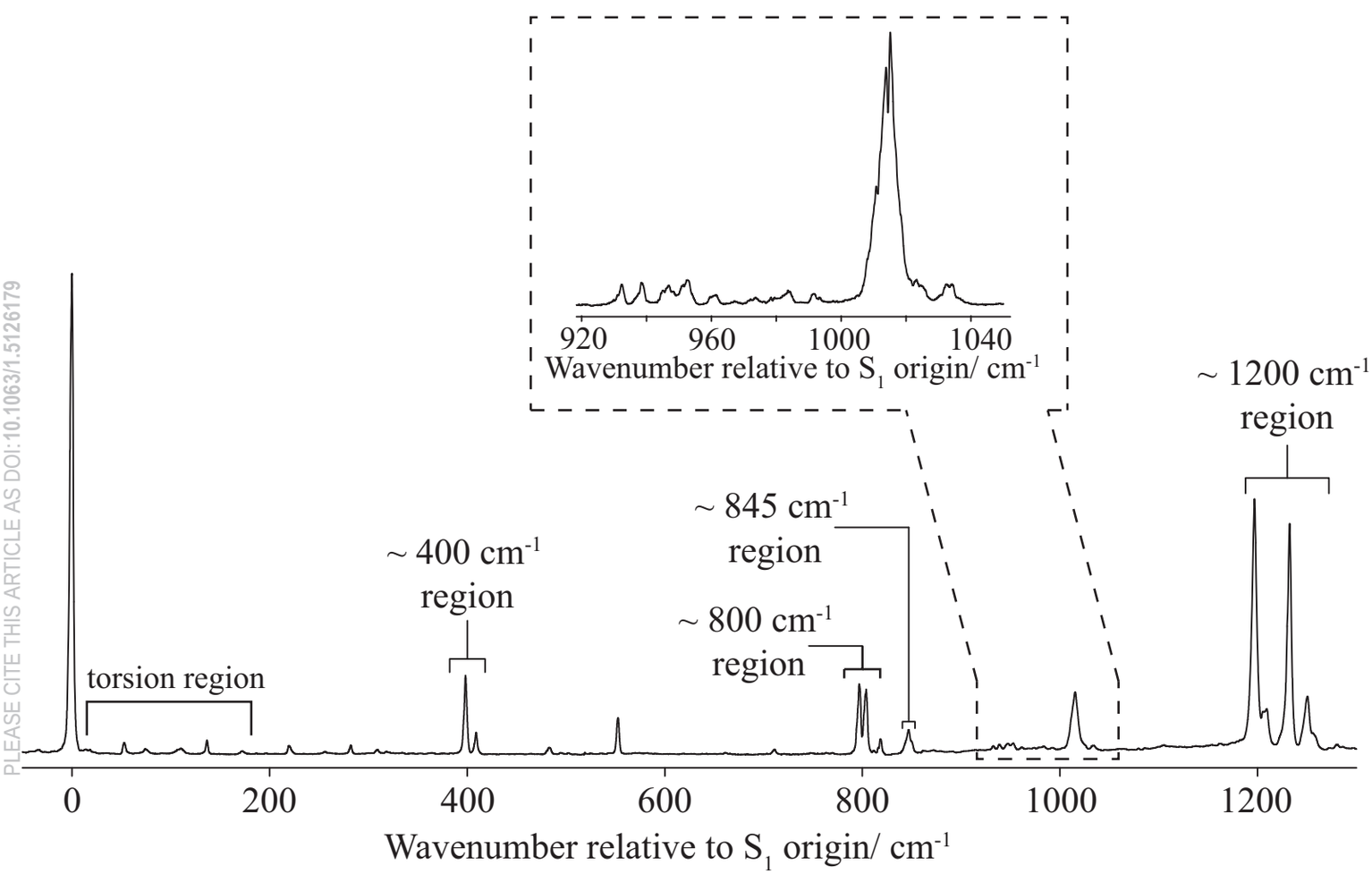

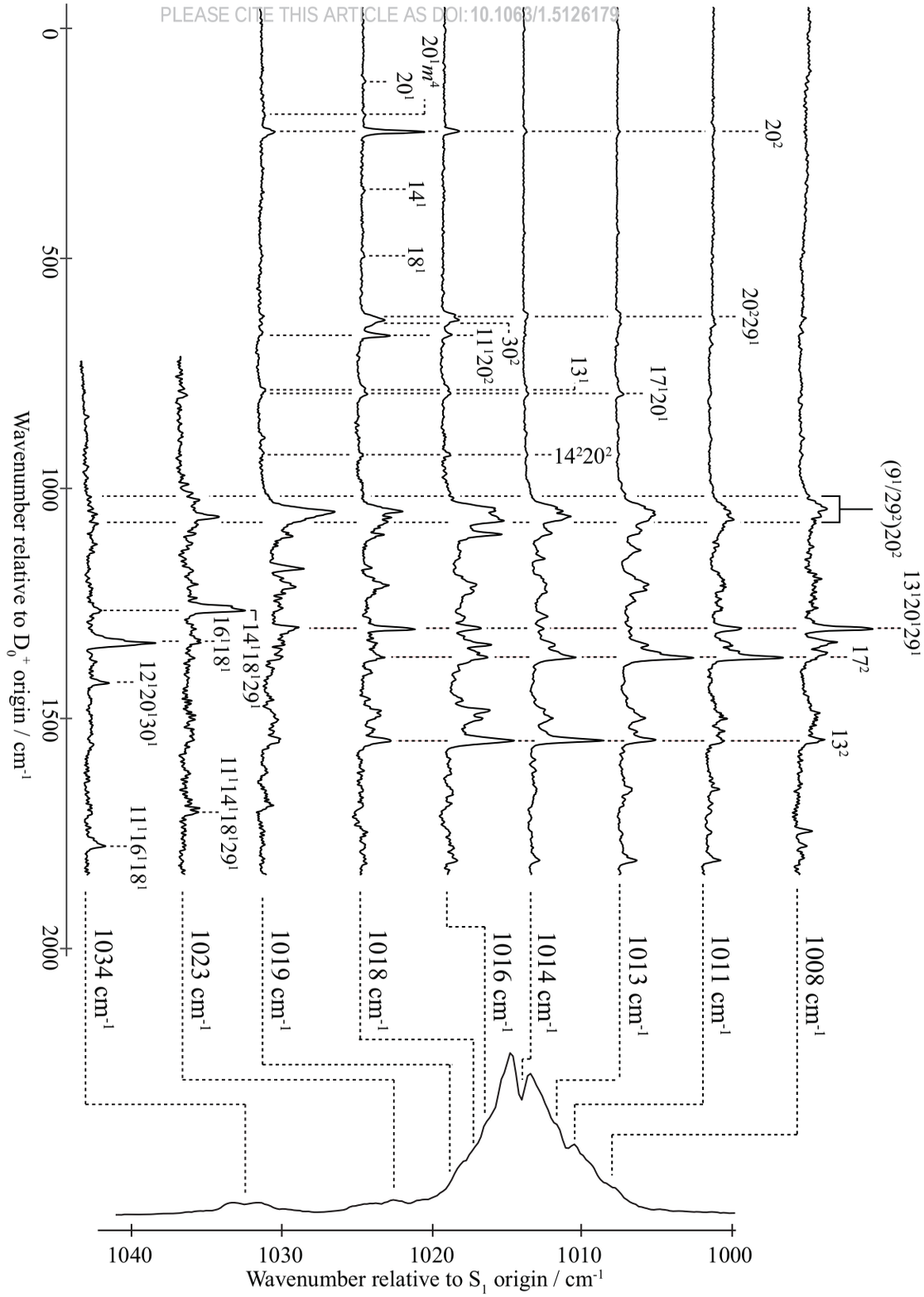

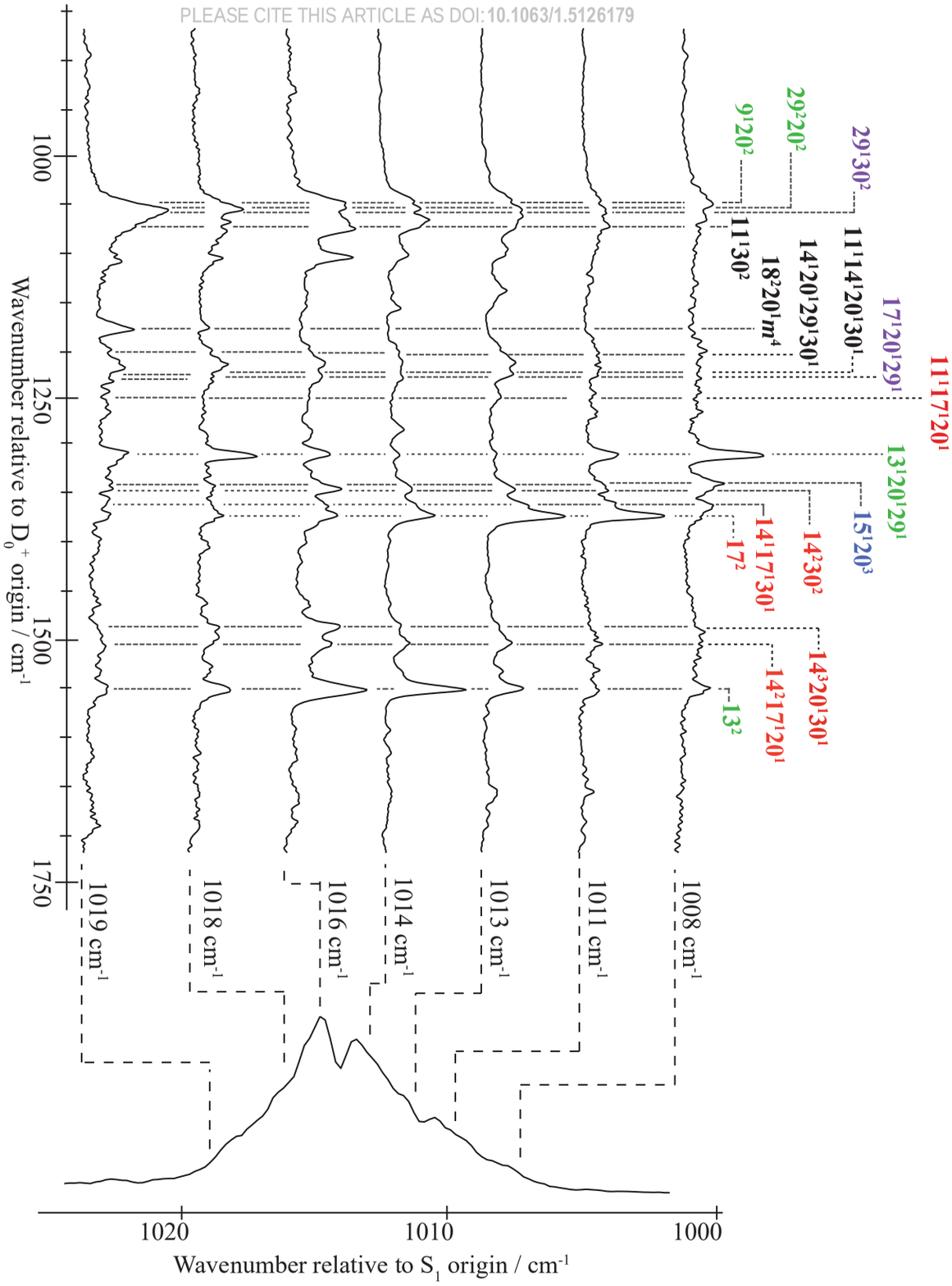

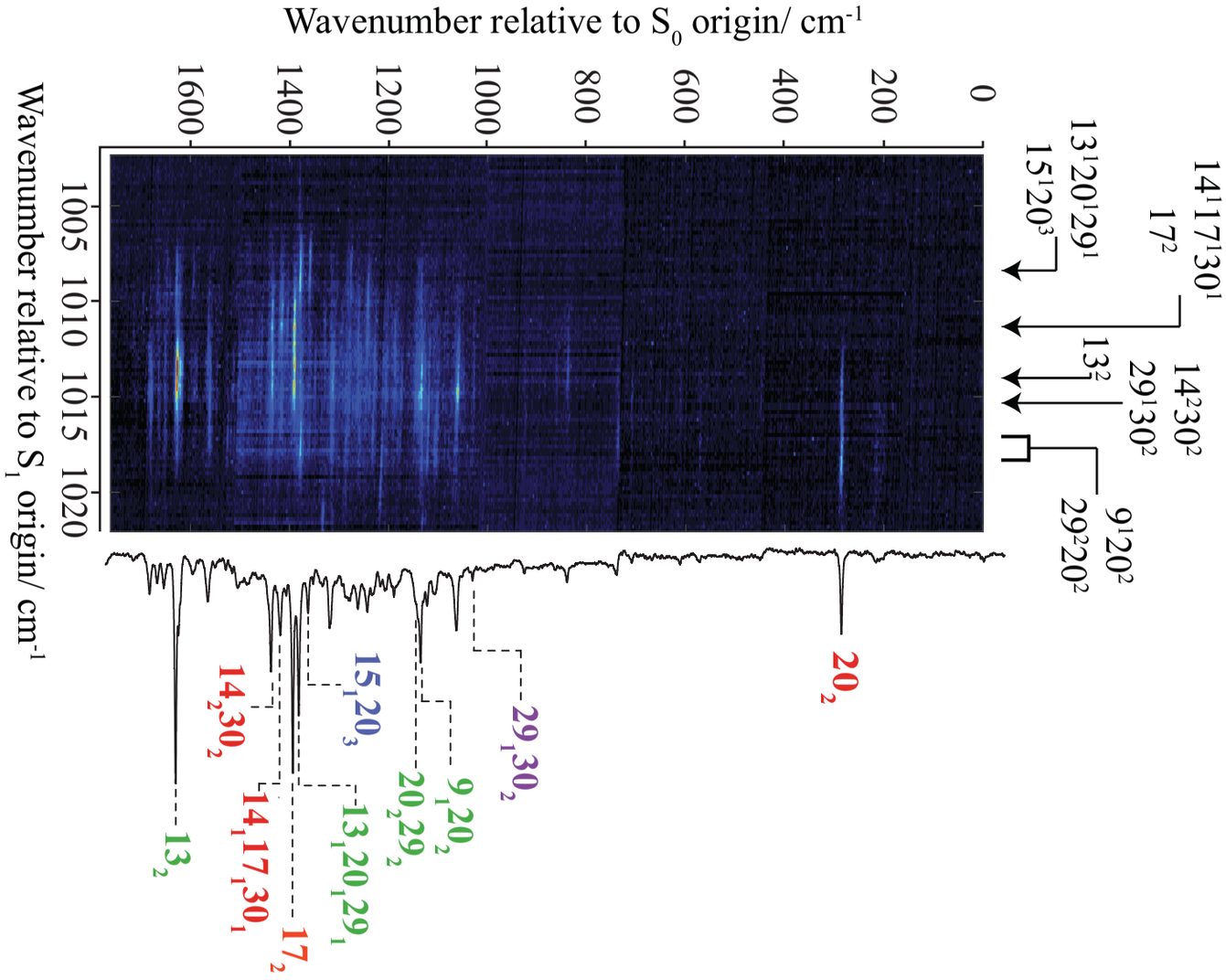

The Journal of Chemical Physics